A Recursive Algorithm for Wideband Temporal Spectrum Sensing

Joseph M. Bruno, *Member, IEEE*, and Brian L. Mark, *Senior Member, IEEE*

***Abstract*—Wideband spectrum sensing techniques determine which portions of a given spectrum band are occupied or idle in the frequency domain. The idle portions represent spectrum holes that can potentially be exploited by secondary or unlicensed users. Existing methods for wideband sensing, however, do not take into account the temporal activity of the primary or licensed users within the spectrum band. We propose an algorithm that identifies primary user activity over a wide spectrum band and provides a statistical characterization of the primary user signals in the band. The algorithm applies hidden Markov modeling to a hierarchically partitioned representation of the spectrum band, together with a recursive tree search. Different from existing wideband sensing algorithms, the proposed wideband temporal sensing method is able to accurately detect spectrum holes even in the presence of bursting primary user signals. Moreover, hidden Markov modeling of the primary user signals enables the accurate detection and prediction of primary user activity over time. Numerical results demonstrate the significant performance gain of the proposed algorithm over existing wideband spectrum sensing algorithms, particularly in the presence of low duty-cycle primary user signals.**

***Index Terms*—Cognitive radio, spectrum sensing, wideband, hidden Markov model**

I. Introduction

Due to the rapidly increasing demand for capacity in wireless networks, radio frequency (RF) spectrum access becomes more precious every day. However, it has been shown that fixed frequency allocations have left large portions of the RF spectrum underutilized [2]. Cognitive radio aims to increase utilization of those bands without disruption to the licensed or primary user [3]. In order to maximize capacity and minimize service disruptions to the primary user (PU), a cognitive secondary user (SU) must employ sophisticated sensing techniques to accurately detect or anticipate the presence or absence of a PU signal in a spectrum band.

Most of the early work on spectrum sensing focused on a narrowband channel, where the PU signal is assumed to be either active or idle at all times. Well-known detection algorithms for narrowband sensing include energy detection, cyclostationary feature detection, and matched filter detection [4]. The energy detector is the simplest of the narrowband detectors and requires no a priori knowledge of the channel, but it performs poorly in the case of low signal-to-noise ratio (SNR). The most sensitive of the listed sensing algorithms is the matched filter, which requires a priori knowledge of the the PU waveform, but can detect PU activity at very low SNR. Cyclostationary feature detection lies between the matched filter and energy detector in terms of performance at low SNR, but incurs significant computational cost and long integration windows. Cyclostationary detector performance is degraded in the case of low PU duty cycle [5].

In wideband spectrum sensing, several PUs may occupy portions of a wide frequency band, but the center frequency and bandwidth of each PU channel are assumed to be unknown. A special case of wideband sensing, often referred to as multiband spectrum sensing, operates under the assumption that the PU channel spectrum parameters are known. Wideband sensing has been studied in a number of papers under the assumption that the PU state is either on or off at all times [6]–[13]. In other words, the temporal dynamics of the PUs are not taken into account in the prior work on wideband sensing. The wideband sensing techniques developed in these works are based on energy detection, edge detection, or cyclostationary feature detection. To reduce the sampling rate required for estimating the power spectral density over a wide frequency band, compressive sensing techniques have been proposed in [14] and applied to wideband sensing based on edge detection as in [12].

Temporal spectrum sensing, which takes into account the dynamic behavior of the PU, has been studied primarily in the narrowband setting. Given that many modern waveforms employ some sort of time division multiple access (TDMA), spectrum sensing algorithms that incorporate a dynamic PU model, such as [15], are highly desirable. Hidden Markov models (HMMs) have been proposed to characterize the dynamic behavior of the PU and predict future temporal spectrum holes on a narrowband channel. The underlying process of the HMM represents the state of the PU, which can be detected only indirectly through the observable process [16], [17]. In [16], a finite alphabet HMM is assumed. In [17], the observable process is conditionally Gaussian given the underlying state to model the effect of lognormal shadowing and other channel impairments. The HMM itself is extended to a hidden bivariate Markov model, which allows for modeling a much more general class of PU state sojourn time distributions. Modeling of PU activity as a Markov process has also been extended to the multiband case, where the allocation of total sensing time among multiple known bands has been studied [18]. A multichannel MAC (medium access control) is proposed in [19], where the PU channels are modeled as

Manuscript received March 1, 2017; revised July 20, 2017; accepted August 27, 2017. This work was supported in part by the U.S. National Science Foundation under Grants CNS-1205453, and CNS-1421869. A preliminary version of this work was presented in [1]. The editor coordinating the review of this paper and approving it for publication was C.-X. Wang.

J. M. Bruno is currently with the Johns Hopkins Applied Physics Lab (e-mail: jbruno2@gmu.edu).

B. L. Mark is with the Dept. of Electrical and Computer Engineering, George Mason University, Fairfax, VA 22030 (e-mail: bmark@gmu.edu).

Markov on-off processes. In [18], [19], the PU state is assumed to be directly observable, such that the channel impairments are not taken into account.

To our knowledge, there has been very little work on spectrum sensing jointly in time and over a wide frequency band. Narrowband or multiband temporal sensing algorithms require prior knowledge of the locations of the PU channels within a spectrum band, while wideband sensing algorithms proposed in the literature assume that the PUs are static, i.e., they are on at all times. In this paper, we develop a framework for *wideband temporal* sensing, which tracks dynamic PU signal activity in both time and frequency by segmenting the spectrum band into smaller subbands. We apply an HMM-based temporal sensing algorithm to each of the channels, allowing for detection of PUs with low duty cycle in the wideband regime. We model the set of subbands as a balanced binary tree and perform a recursive search for spectrum holes. Adjacent spectrum holes are merged into a single spectrum hole. This process is carried out in a recursive manner with the objective of determining a minimal set of PU channels, of possibly different bandwidths, that spans all PU signals in the spectrum band. In effect, our approach reduces the wideband temporal sensing problem into a multiband sensing problem.

Existing wideband sensing techniques generally compute the power spectral density for a given spectrum band by averaging power estimates over a time window. The implicit assumption is that the power spectral density remains static, at least for the duration of the averaging window. However, such wideband sensing algorithms may fail to detect PUs that change state dynamically over time, and are especially inadequate in the presence of PUs with low duty cycle. Our experimental results demonstrate that the proposed scheme for wideband temporal sensing significantly outperforms existing wideband sensing approaches, particularly in the presence of PU signals with low duty cycles. More importantly, the incumbent techniques for wideband sensing are not able to fully exploit temporal spectrum holes for dynamic spectrum access, since they do not model the temporal behavior of spectrum activity.

The main contribution of this paper is a systematic framework and computationally efficient algorithms for wideband sensing that explicitly take into account the temporal activity of dynamic PUs. The proposed wideband temporal sensing algorithm provides an efficient and practical solution to a problem that has not previously been addressed in the literature on spectrum sensing. The primary innovations of our approach consist of (1) application of hidden Markov modeling to a partitioned representation of the spectrum band, (2) a recursive tree search for finding and aggregating spectrum holes to identify dynamic PU signals in the given spectrum band. The proposed wideband temporal sensing algorithm results in the identification of a minimal set of PU channels that spans the spectrum band, together with HMM parameters characterizing each of the channels in the set. The HMM parameters can then be used to perform temporal spectrum sensing of the identified channels as in [17]. In particular, the statistical characterization of PUs signals by HMMs (or more generally, the hidden bivariate Markov models in [17]) enables accurate detection and prediction of PU activity. This opens the door for secondary users to exploit spectrum holes occurring both in time and frequency.

The key technical challenge in extending the narrowband spectrum sensing algorithm in [17] lies in identifying the unknown PU channel boundaries (or equivalently, the spectrum holes), and characterizing each of the identified PU channels by an HMM parameter in a computationally efficient manner. This requires an efficient tree search procedure combined with HMM parameter estimation applied to a large set of subbands, as well as a fast and accurate method for aggregating the subbands into spectrum holes. The remainder of the paper is organized as follows. In Section II, we discuss and evaluate the performance of two existing wideband spectrum sensing techniques. In Section III, we introduce a system model for a dynamic PU under channel fading and noise impairments. In Section IV, we develop our proposed recursive tree search algorithm to perform wideband temporal spectrum sensing. In Section V we describe the simulation that was used to compare the proposed algorithm to existing algorithms and present numerical results. Concluding remarks are given in Section VI.

II. Comparison of Wideband Spectrum Sensing Techniques

In the wideband spectrum sensing scenario, an SU must sense an entire band and determine channel boundaries. The bandwidth that must be sensed can vary from the order of 1 MHz to 1 GHz. Wideband spectrum sensing is required if the SU cannot leverage any external information about channel allocation. An example of external channel information is provided by the television bands in the United States, where 6 MHz channels have been clearly defined by the Federal Communications Commission [20]. An SU can perform wideband sensing during initialization and then revert to multiband or narrowband sensing during normal operation.

To evaluate the incumbent wideband sensing techniques, orthogonal frequency division multiplexing (OFDM) and Gaussian minimum shift keying (GMSK) are used. OFDM signals exhibit sharp rectangular band edges, whereas GMSK signals exhibit gradual sloping band edges. Because these signals represent extremes in the boundaries between signals, the performance of the evaluated detectors on other modulations should fall somewhere between that of OFDM and GMSK. Not only do they have drastically different band edges, but GMSK and OFDM are pervasive in modern wireless standards such as GSM (GMSK), WiFi (OFDM), and LTE (OFDM).

We assume that a channel can take on one of two states: an idle state, in which the PU does not transmit, and an active state, in which the PU transmits. We denote idle and active states by 0 and 1, respectively. For a given channel, the steady-state probabilities that the PU is idle and active are denoted, respectively, by π_0 and π_1. The duty-cycle of the channel corresponds to π_1 stated as a percent value.

A. Wideband Energy Detector

A very simple wideband sensing technique is a wideband energy detector [21], [22] where the SU estimates the power

spectral density (PSD) over the entire band and employs an energy threshold to determine PU activity. Many PSD frames may be averaged to increase reliability. This simple algorithm has many limitations. Like all energy detectors in additive white Gaussian noise (AWGN), this technique has limited sensitivity, and performance is severely degraded at low SNR. Furthermore, the sensitivity of the averaged PSD estimate will be degraded in the case where the PU exhibits dynamic behavior. If the PU employs a bursting signal or frequency hopping, idle periods may be averaged together with active periods, which compromises the estimator's accuracy.

Figures 1 and 2 qualitatively show the sensing results of a frequency-domain energy detector for OFDM and GMSK signals, respectively. Shaded areas represent detected spectrum holes. All of the signals shown have an SNR of 10 dB, but for the bursting signals, the magnitude of the PSD estimate decreases with the duty cycle. This decreased PSD magnitude degrades the performance of the energy detector for both modulation schemes.

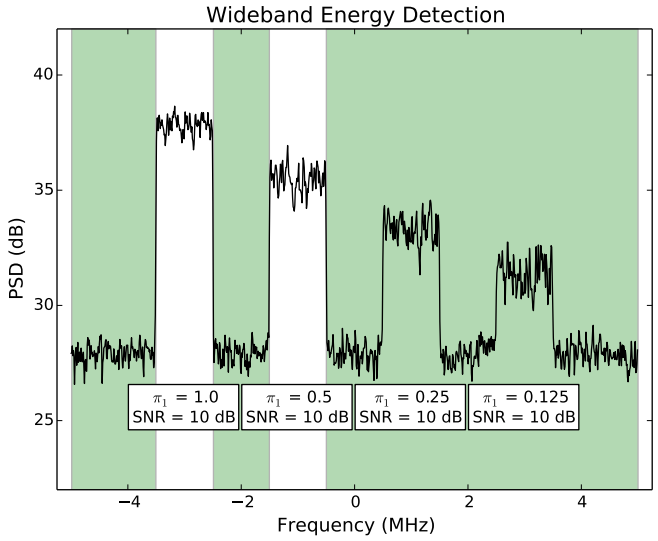

Fig. 1. Results of a wideband energy detector for OFDM signals with 10 dB SNR and 100%, 50%, 25%, and 12.5% duty cycles.

Performing a maximum hold operation rather than averaging PSD frames has been proposed for detecting dynamic PUs [23]. Maximum hold detectors have identical complexity and memory requirements to averaging detectors with the same number of frequency bins and sensing duration. However, maximum hold energy detectors are outperformed by averaging detectors in low SNR [23]. Furthermore, maximum hold energy detectors can actually cause an increased probability of false alarm as observation lengths are increased due to increased likelihood of an abnormally high noise power during the sensing interval. These two shortfalls make maximum hold energy detectors inadequate for cognitive radio applications and motivate the need for a wideband sensing algorithm that adequately detects dynamic PU activity.

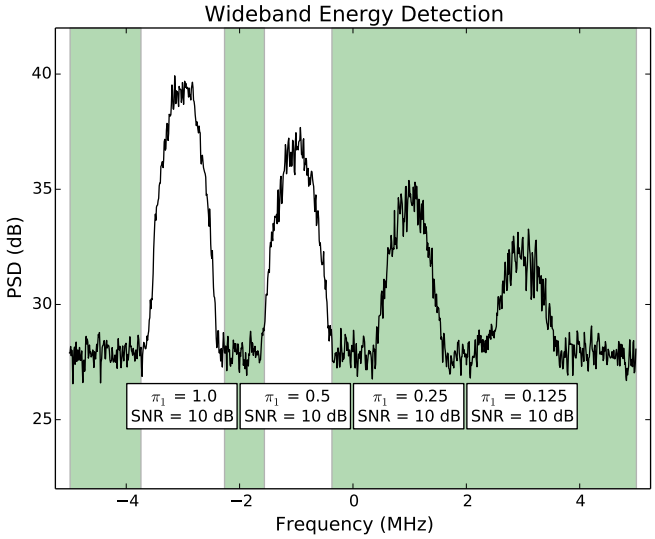

Fig. 2. Results of a wideband energy detector for GMSK signals with 10 dB SNR and 100%, 50%, 25%, and 12.5% duty cycles.

B. Wideband Edge Detector

A popular approach to wideband spectrum sensing involves performing frequency-domain edge detection to determine channel boundaries. The edge detector proposed in [12] uses the continuous wavelet transform to decompose edge detection into multiple resolutions and then multiplies the resolutions together, which has a beneficial effect of reducing the noise. While edge detectors do offer an improvement over energy detectors in terms of performance at low SNR, they come with several limitations. Most importantly, edge detectors require that PU signals have sharp transitions in the frequency domain. This allows them to work well with the rectangular spectra of signals like OFDM (see Fig. 3) and quadrature amplitude modulation (QAM) with low excess bandwidth, but edge detectors tend to perform poorly on signals with gradual slopes on their band edges, such as QAM with large excess bandwidth and GMSK.

The performance of an edge detector using the multi-resolution enhancements from [12] is shown for GMSK in Fig. 4. The figure shows that wideband edge detectors suffer from the same shortfall as wideband energy detectors in that they are also degraded by dynamic behavior of the PU. Because received signal samples from both idle and active cycles are averaged into the PU detector, the performance of the detector deteriorates with decreasing duty cycle of the PU.

C. Compressive Sensing

A class of sensing algorithms known as compressive sensing has been proposed for surveying very wide bandwidths with sub-Nyquist sampling rates. Because much of the radio spectrum is underutilized, available bands may be represented as a sparse dataset, and depending on the sparsity order of the dataset, the wideband signal may be sensed at a fraction of the Nyquist rate [24]. To perform sub-Nyquist sampling, the signal time series is divided into length-M blocks of Nyquist-rate samples, of which K samples are kept, giving an under-

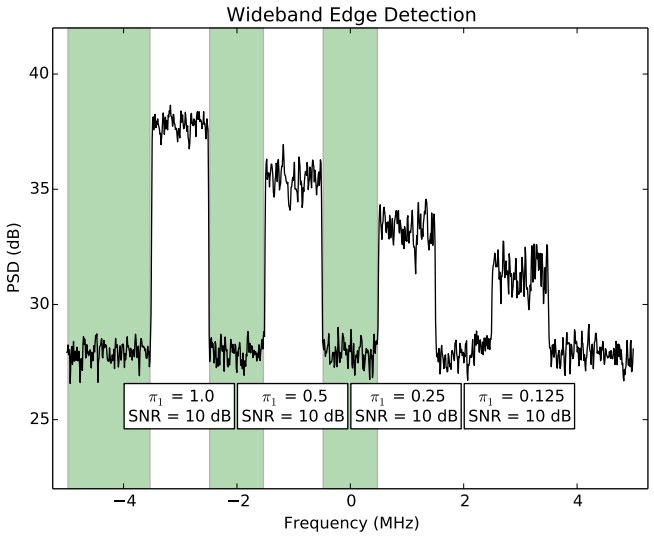

Fig. 3. Results of a wideband edge detector for OFDM signals with 10 dB SNR and 100%, 50%, 25%, and 12.5% duty cycles.

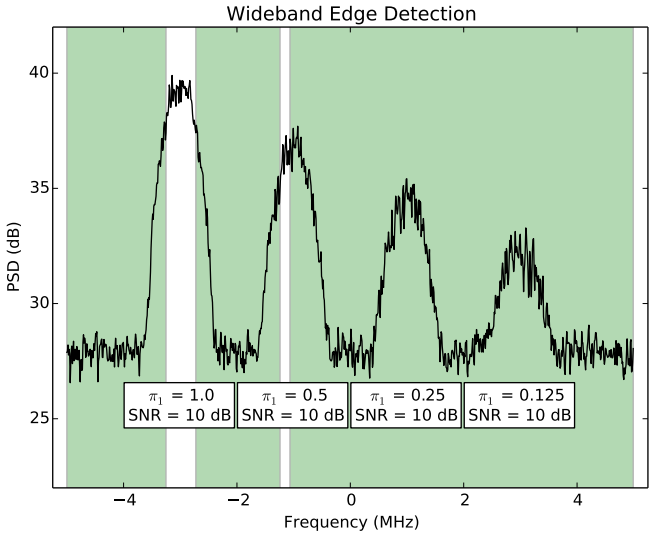

Fig. 4. Results of a wideband edge detector for GMSK signals with 10 dB SNR and 100%, 50%, 25%, and 12.5% duty cycles.

sampling fraction of K/M. Reconstruction of the sparse PSD from the undersampled data is accomplished by solving for a linear inverse, which in the sparse case requires a numerical solution [14]. To select an appropriate undersampling fraction, the cognitive receiver must have prior knowledge of the PU sparsity order. An online sparsity estimator has been proposed in [25] that can quickly determine an undersampling ratio.

Although compressive sensing can be utilized to sense much wider bandwidths than can be done with traditional analog to digital conversion hardware, the result of compressive sensing typically involves a static PSD estimate. For example, in [14], the estimated sparse PSD is analyzed with the wavelet-based edge detector proposed in [12]. Since current compressive sensing methods rely on a static PSD estimate, the presence of low duty-cycle PU signals can drastically reduce the detector sensitivity. In [24] it is stated that current compressive sensing cannot be used to properly handle sparsity in time and space. Although our proposed sensing algorithm requires sampling at the Nyquist rate and therefore cannot be used for ultra wideband sensing, its success does not rely on signal sparsity in any domain, and it more flexibly detects bursting signals by leveraging time-domain sensing methods.

III. System Model

Over a spectrum band of total width B Hz, an unknown number of PU signals are operating with temporal duty cycles in the range 0 to 100 percent. Each PU signal has an unknown center frequency, f_c Hz, and bandwidth, W Hz. It is assumed that PU channels are non-overlapping in frequency. In practice, the PU channels would typically be separated by guard bands to avoid interference with each other. The channel over which the i^{th} PU is observed is assumed to be flat Rayleigh fading with parameter $\sigma_{f,i}$ combined with additive white Gaussian noise (AWGN), defined by the circularly symmetric complex normal distribution $\mathcal{C}\left(0, \sigma_{n,i}^2\right)$. The mean SNR of the received signal on channel i, given that the PU is transmitting is

$$\overline{\mathrm{SNR}}_i = \frac{\sigma_{f,i}^2}{\sigma_{n,i}^2}. \tag{1}$$

A. PU Traffic Model

A PU may be transmitting or idle at any given time. The state of the i^{th} PU, denoted by random variable X_i, may alternate between the idle state $X_i = 0$, where the PU is not transmitting, and the busy state $X_i = 1$, where the PU is transmitting. The k^{th} PU state is denoted $X_{i,k}$. Each PU is modelled by a discrete-time Markov chain with transition matrix G_i and initial distribution ν_i, defined as

$$G_i = \left[g_{i,ab} : a, b \in \{0, 1\}\right], \tag{2}$$

$$g_{i,ab} = \mathrm{P}\left(X_{i,k} = a, X_{i,k+1} = b\right), \tag{3}$$

$$\nu_{i,0} = \mathrm{P}\left(X_{i,1} = 0\right), v_{i,1} = \mathrm{P}\left(X_{i,1} = 1\right). \tag{4}$$

B. Cognitive Receiver Model

1) Received Wideband Signal: A transmitting PU will generate a bandpass signal $\tilde{t}_{i,k}$. The transmitted signal for PU i at any time k is

$$t_{i,k} = \tilde{t}_{i,k} \cdot 1_{\{X_{i,k}=1\}}, \tag{5}$$

where 1_A is the indicator function on the set or condition A. The i^{th} PU signal is multiplied at time k by a fading signal $f_{i,k} \sim \mathcal{C}\left(0, \sigma_{f,i}^2\right)$. All M PU signals are received simultaneously and added to the noise signal $n_k \sim \mathcal{C}\left(0, \sigma_{n,i}^2\right)$. The received wideband signal is represented by a sequence of samples $z_{wb}^n = \{z_{wb,1}, \ldots, z_{wb,n}\}$, where $z_{wb,k}$, the k^{th} I-Q sample from the wideband channel, is defined as

$$z_{wb,k} = \sum_{i=1}^{M} t_{i,k} f_{i,k} + n_k. \tag{6}$$

2) Channelized Received Signal: The SU will divide the wideband received signal into J narrowband subchannels. Initially this division must be done arbitrarily, but after wideband sensing, the set of subchannels should describe all PU statistics as well as the statistics of the spectrum holes between PU signals. The j^{th} subband is denoted z_j.

3) Energy Detected Signal: For spectrum sensing, the channelized narrowband signals are processed with an averaging energy detector, which estimates the power of each sample and averages N_{avg} samples together. The resulting random variable for the received energy in subchannel j is denoted by Y_j, and the sequence of energy estimates for subchannel j is denoted $y_j^n = \{y_{j,1}, \ldots, y_{j,n}\}$. The k^{th} sample in the energy detection sequence, $y_{j,k}$, is defined as

$$y_{j,k} = \frac{1}{N_{\text{avg}}} \sum_{i=1}^{N_{\text{avg}}} |z_{j,(k-1)N_{\text{avg}}+i}|^2. \tag{7}$$

An SU will need to detect slow changes in PU state to properly leverage spectrum holes, and because of this, we assume that the probability of a state change occurring during the energy estimation of a single sample to be minimal. Therefore, we assume that during an energy detection window the samples of y_j are independent, identically distributed (IID). For relatively large N_{avg}, Y will approach a normal random variable due to the Central Limit Theorem. If Y_j represents the energy estimates of a subchannel with PU i, the k^{th} sample from the received narrowband signal, z_j, will be generated by a random variable with conditional distribution

$$z_{j,k} \sim \begin{cases} \mathcal{C}\left(0, \sigma_{n,i}^2\right), & X_{i,k} = 0, \\ \mathcal{C}\left(0, \sigma_{f,i}^2 + \sigma_{n,i}^2\right), & X_{i,k} = 1. \end{cases} \tag{8}$$

The resulting energy estimates, $y_{j,k}$, will be scaled chi-squared random variables with $2N$ degrees of freedom. We will denote a chi-squared distribution with D degrees of freedom $\mathcal{X}^2(D)$. The conditional distribution of the energy detector is therefore

$$y_{j,k} \sim \begin{cases} \frac{\sigma_{n,i}^2}{N_{\text{avg}}} \mathcal{X}^2\left(2N_{\text{avg}}\right), & X_{i,k} = 0, \\ \frac{\sigma_{f,i}^2 + \sigma_{n,i}^2}{N_{\text{avg}}} \mathcal{X}^2\left(2N_{\text{avg}}\right), & X_{i,k} = 1. \end{cases} \tag{9}$$

The mean and variance of a chi-squared distribution with D degrees of freedom are D and $2D$ respectively. Assuming that N_{avg} is sufficiently large, $y_{j,k}$ will be conditionally normal with distribution

$$y_{j,k} \sim \begin{cases} \mathcal{N}\left(2\sigma_{n,i}^2, \frac{4\sigma_{n,i}^4}{N_{\text{avg}}}\right), & X_{i,k} = 0, \\ \mathcal{N}\left(2\sigma_{f,i}^2 + 2\sigma_{n,i}^2, \frac{4\left(\sigma_{f,i}^2 + \sigma_{n,i}^2\right)^2}{N_{\text{avg}}}\right), & X_{i,k} = 1. \end{cases} \tag{10}$$

IV. Recursive Algorithm for Wideband Temporal Sensing

In this section, we propose an approach that extends narrowband temporal sensing techniques to the wideband scenario. Narrowband techniques that use HMMs [26] to model the dynamic behavior of the PU are leveraged to overcome the limitations of current wideband spectrum detectors. In particular, we shall rely on the narrowband sensing approach in [17], which is based on a generalization of the HMM referred to as a hidden bivariate Markov model (HBMM). For simplicity, we shall restrict ourselves to the HMM characterization of a PU channel, but our approach can straightforwardly accommodate the HBMM. The proposed wideband search algorithm may also be adapted to leverage other narrowband sensing techniques for various special purposes. For example, for channels with high duty cycle but very low SNR, the proposed wideband algorithm could be adapted to work with a cyclostationary detector.

A. Wideband Tree Search

In our proposed algorithm for wideband temporal sensing, the spectrum band is organized as a balanced binary tree, where each node has two child nodes representing the upper and lower halves of the band. The band is recursively divided into smaller pieces as depth increases [27]. A maximum depth is selected based on a desired resolution for the wideband sensing algorithm. The depth of the tree is given by $d = \lceil \log_2(W_0/W_r) \rceil$, where W_0 is the bandwidth, and W_r is the maximum frequency resolution. The resulting number of channels at the finest resolution, N_c, is given by $N_c = 2^d$. The frequency resolution W_r must be selected by the implementer, as a smaller sensing resolution allows finer spectral components to be observed, but increases computational complexity resulting from increased N_c, as shown in Eq. (31). The division of a band into subbands using a balanced binary tree is shown in Fig 5.

The algorithm recursively divides a given channel in half until the desired resolution is reached. An inorder traversal, a recursive search where child nodes are visited before parent nodes [27], is performed on the balanced binary tree that is used to model the spectrum band. At the highest resolution, each subband or channel is sensed using a narrowband temporal spectrum sensing technique based on hidden Markov mdoels.

B. Channel Selection

A channelizer must be employed to divide the wideband channel into 2^d subbands, where d is the search tree depth. A conceptually simple channelizer is a bank of digital downconverters (DDCs), with one DDC for each subband. A diagram for a simple DDC is shown in Fig. 6. Given a sequence $\{a_k\}_{k=1}^{\infty}$, we use the convenient notations $a_k^n = \{a_k, \ldots, a_n\}$ and $a^n = \{a_1, \ldots, a_n\}$. The received wideband signal can then be represented by a sequence of samples $z_{\text{wb}}^n = \{z_{\text{wb},1}, \ldots, z_{\text{wb},n}\}$, where $z_{\text{wb},k}$ denotes the kth I-Q sample from the wideband channel. When the received wideband signal z_{wb}^n is passed into the DDC, it will first be mixed down by center frequency f_c, such that the center of the band of interest is now at baseband. The baseband signal is next lowpass filtered with FIR taps $h(n)$ to isolate the band of interest. Finally, the signal is decimated by rate dec, keeping 1

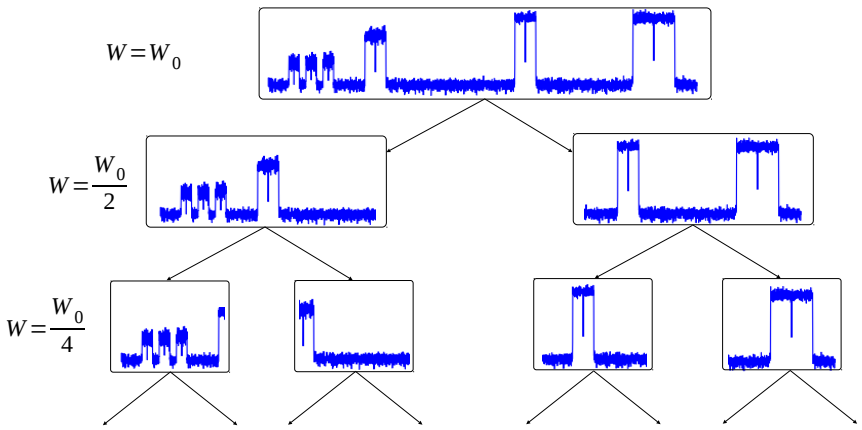

Fig. 5. A wideband channel, i.e., a spectrum band with bandwidth W_0, organized into a balanced binary tree.

sample out of every dec. The channelized narrowband signal is denoted z^n.

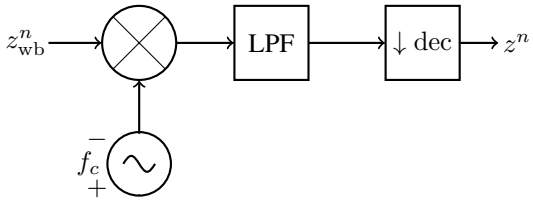

Fig. 6. A simple digital downconvertor for signal channelization.

Because all subbands are eventually channelized by the recursive search, a frequency-domain channelizer using the fast Fourier transform (FFT) [28], [29] can substantially reduce the computational cost of the channel selection. Frequency-domain channelizers have been studied in detail [28], and while faster computationally, use of a frequency-domain channelizer would not alter the outcome of the proposed algorithm. Therefore, for the sake of simpler algorithm description, a simple filter-and-decimate channelizer was discussed above. For spectrum sensing, the channelized narrowband signals are processed with an averaging energy detector, which estimates the power of each sample and averages N_{avg} samples together. The received power estimate of the sample z_k in linear units, e.g., mW, is denoted y_k, and is calculated as follows:

$$y_k = \frac{1}{N_{\text{avg}}} \sum_{i=1}^{N_{\text{avg}}} |z_{k+i}|^2 . \tag{11}$$

C. Hidden Markov Modeling for Narrowband Sensing

Although the recursive tree search that we propose can leverage a variety of narrowband techniques, we are addressing the specific issue of PU dynamics such as bursting and frequency hopping. An HMM is used to model the channel dynamics, assuming a lognormal shadowing model. In [17], [30], a more general form of HMM referred to as a hidden bivariate Markov model (HBMM) is applied to narrowband temporal spectrum sensing. An extension of the Baum-Welch algorithm was developed in [17] for estimating the parameter of a HBMM. The Baum-Welch algorithm is an offline algorithm, which iteratively produces a sequence of parameter estimates with increasing likelihood, based on a given an observation sequence. An online parameter estimation algorithm for the HBMM was developed in [30]. Since the focus of the present paper is on wideband sensing, we will restrict ourselves to the simpler HMM and the standard Baum-Welch algorithm for parameter estimation.

We use P to denote a generic probability measure and P_ϕ to denote a probability measure that depends on a parameter ϕ. Similarly, we use p and p_ϕ to denote a probability density function or probability mass function as appropriate. In the notation $p(x_k) = P(X_k = x_k)$, the lowercase symbol x_k on the left-hand side implicitly implies the associated random variable represented by the uppercase symbol X_k. The HMM, denoted by (Y, X), consists of an observable sequence of received signal strengths, $Y = \{Y_k\}_{k=1}^{\infty}$, and an underlying or hidden state sequence $X = \{X_k\}_{k=1}^{\infty}$, which is assumed to be a discrete-time Markov chain. At time k, Y_k represents the averaged received signal power, after processing, in linear units (mW) and X_k represents the state of the PU, i.e., $X_k = 0$ when the PU is idle and $X_k = 1$ when the PU is active. Assuming a standard path loss plus Rayleigh fading model, the received signal power Y_k can be expressed as follows (cf. [30]):

$$Y_k = \begin{cases} \mu_0 + \epsilon_0, & X_k = 0, \\ \mu_1 + \epsilon_1, & X_k = 1, \end{cases} \tag{12}$$

where μ_a represents the mean received signal power when the PU is in state $a \in \{0, 1\}$, and ϵ_a is a zero-mean Gaussian random variable with standard deviation σ_a, which may represent impairments such as receiver noise, fading, or shadowing. A similar model was validated empirically in the context of temporal spectrum sensing of a narrowband channel in [17]. In this paper, Rayleigh fading was simulated, resulting in Eq. (10) for Y_k.

Let $G = [g_{ab} : \ a, b \in \{0, 1\}]$ denote the transition matrix of the underlying Markov chain X, where g_{ab} denotes the transition probability from state a to state b. Let $\nu = [\nu_0, \nu_1]$ denote the initial state probability distribution, where

$$\nu_1 = P(X_1 = 0), \ \nu_2 = P(X_1 = 1).$$

The parameter of the HMM is given by $\phi = (\nu, G, \mu, R)$, where $\mu = [\mu_0, \mu_1]$ and $R = [\sigma_0^2, \sigma_1^2]$.

D. Baum-Welch Algorithm and MAP Detector

The Baum-Welch algorithm [31] is applied to obtain an estimate of the HMM parameter for a given channel, as part of the recursive tree search. The input to the algorithm is an initial parameter estimate ϕ^s and an observed sequence y^n obtained from the channel. Starting with the initial estimate, $\hat{\phi}_0 = \phi^s$, the ιth iteration ($\iota \geq 1$) of the algorithm produces a new estimate $\hat{\phi}_\iota$ with likelihood greater than or equal to that of $\hat{\phi}_{\iota-1}$. Each iteration of the algorithm involves the computation of forward and backward recursions [26, Section V.A].

Let ϕ denote the current parameter estimate at the start of an iteration of the Baum-Welch algorithm. Define a diagonal matrix

$$B(y_k) = \mathrm{diag}\{p_\phi(y_k \mid x_k = 0), p_\phi(y_k \mid x_k = 1)\}.$$

We denote the (scaled) forward and backward variables by $\bar{\alpha}(x_k, y^k)$ and $\bar{\beta}(y_{k+1}^n \mid x_k)$, respectively. The forward vector is defined as a row vector

$$\bar{\alpha}_k = [\bar{\alpha}(x_k = 0, y^k), \bar{\alpha}(x_k = 1, y^k)],$$

while the backward vector is defined as a column vector

$$\bar{\beta}_k = [\bar{\beta}(y_{k+1}^n \mid x_k = 0), \bar{\beta}(y_{k+1}^n \mid x_k = 1)]',$$

where $'$ denotes matrix transpose. Let $\mathbf{1}$ denote a column vector of all ones, of appropriate dimension depending on the context. The forward recursion is given by

$$\bar{\alpha}_1 = \frac{\nu B(y_1)}{c_1}, \quad \bar{\alpha}_k = \frac{\bar{\alpha}_{k-1} G B(y_k)}{c_k}, \ k = 2, \ldots, n, \quad (13)$$

where $c_1 = \pi B(y_1)\mathbf{1}$, and $c_k = \bar{\alpha}_{k-1} G B(y_k)\mathbf{1}$ for $k = 1, \ldots, n$. The forward variables have the following interpretation: $\bar{\alpha}(x_k, y^k) = p(x_k \mid y^k)$. The backward recursion is given by

$$\bar{\beta}_n = \mathbf{1}; \quad \bar{\beta}_n = G B(y_{n+1}) \frac{\bar{\beta}_{n+1}}{c_n}, \ k = n-1, \ldots, 1. \quad (14)$$

The state conditional probability can be obtained from

$$p_\phi(x_k \mid y^n) = \bar{\alpha}(x_k, y^k)\bar{\beta}(y_{k+1}^n \mid x_k). \quad (15)$$

The joint state conditional probability can be calculated as follows:

$$p_\phi(x_{k-1}, x_k \mid y^n) = \frac{\bar{\alpha}(x_{k-1}, y^{k-1})\bar{\beta}(y_{k+1}^n \mid x_k) g_{x_{k-1},x_k} p_\phi(y_k \mid x_k)}{\sum_{x_{k-1},x_k} \bar{\alpha}(x_{k-1}, y^{k-1})\bar{\beta}(y_{k+1}^n \mid x_k) g_{x_{k-1},x_k} p_\phi(y_k \mid x_k)}. \quad (16)$$

The re-estimation formulas for the new parameter estimate are given in terms of (15) and (16) as follows:

$$\hat{g}_{ab} = \frac{\sum_{k=2}^n p_\phi(x_{k-1} = a, x_k = b \mid y^n)}{\sum_{k=2}^n p_\phi(x_{k-1} = a \mid y^n)},$$

$$\hat{\mu}_a = \frac{\sum_{k=1}^n p_\phi(x_k = a \mid y^n)\ y_n}{\sum_{k=1}^n p_\phi(x_k = a \mid y^n)}, \quad (17)$$

$$\hat{\sigma}_a^2 = \frac{\sum_{k=1}^n p_\phi(x_k = a \mid y^n)\ (y_k - \hat{\mu}_a)^2}{\sum_{k=1}^n p_\phi(x_k = a \mid y^n)}, \quad (18)$$

where $a, b \in \{0, 1\}$.

After the Baum-Welch algorithm converges to a final parameter estimate ϕ, the maximum a posteriori (MAP) decisions may be obtained from the a posteriori state probabilities, as given in (15), as follows:

$$\hat{x}_k = \arg\max_{x_k \in \{0,1\}} p_\phi(x_k \mid y^n). \quad (19)$$

Since the MAP decisions take into account the temporal dynamics of the PU signal, the MAP detector can be significantly more accurate than a standard energy detector (cf. [17]). The MAP detector (19) can be used for online spectrum sensing of the given channel.

E. Channel Usability and Channel Capacity

A heuristic test based on the HMM parameter estimate for a channel is performed to determine whether the channel can be used by the SU. Given the transition matrix G, the stationary state distribution $\pi = [\pi_0, \pi_1]$ can be computed from the equations

$$\pi = \pi G, \ \pi\mathbf{1} = 1. \quad (20)$$

The channel is deemed to be a *hole* if the probability that the PU is idle, π_0, exceeds a threshold $\pi_{\min,0}$ (see Algorithm 1, line 13). Note that π_1 represents the duty cycle of the channel. If the sensed channel is determined to be a hole, the center frequency, bandwidth, MAP decisions on the PU state, and filtered decimated samples of the channel are passed to the parent node in the tree.

Given an estimate of the HMM parameter for a channel, an estimate of the SNR for the channel can be obtained. Let μ_a denote the mean received signal strength in linear units, e.g., mW, for $a = 0, 1$. The SNR estimate is computed as

$$\mathrm{SNR} = \frac{\mu_1 - \mu_0}{\mu_0}. \quad (21)$$

The capacity of the channel can then be estimated using the sensed bandwidth, the estimated SNR, and the stationary distribution of the HMM. The capacity is derived from the capacity for a single user with availability π_0 in a TDMA system [32, Eq. 15.150]. We have defined π_0 as the stationary probability that the PU is not using a given band. With these considerations, the capacity in (bits/s/Hz) is computed as follows:

$$C = \pi_0 \log_2 (1 + \mathrm{SNR}). \quad (22)$$

The proposed estimate for channel capacity does not play a direct role in our algorithm for wideband temporal sensing, but is useful for assessing the potential capacity gains achievable through spectrum sensing.

F. Channel Aggregation

As the algorithm recurses upward through the binary tree depicted in Fig. 5, the parent nodes combine two lists of spectrum holes: one from the lower half of the band, and the other from the upper half of the band. If the highest-frequency hole from the lower band and the lowest-frequency

hole from the upper band are adjacent, the two holes can possibly be combined. The objective of wideband sensing is to determine a minimal set of narrowband PU channels that spans the given spectrum band, which can be sensed independently and shared temporally with SUs during the idle periods of the PUs. To achieve this objective, the adjacent holes will only be combined if they are sufficiently correlated in a statistical sense to be defined shortly. The channel aggregation scheme proposed in this paper is based on the time-domain cross-correlation. The rationale behind doing so is that the resulting narrowband PU channels will be approximately uncorrelated and may therefore be treated as being independent. This enables multiband spectrum sensing techniques to be applied to the set of PU channels obtained via the recursive search procedure. It is important to note that the PU channels are treated as independent from the perspective of the receiver. Thus, in the presence of frequency-selective fading, a single PU signal could appear to the receiver as two or more independent PU channels, requiring tracking of additional PU channels on the receiver side. This would be necessary in this scenario due to the lack of coherence across the true PU channel.

The proposed channel aggregation function, while based on time-domain correlation, must account for dynamic signals. Two perfectly correlated bursting signals will appear uncorrelated during idle periods, since white noise signals are inherently uncorrelated. The MAP detector given by (19) can be used to determine the periods during which the PUs are most likely idle for both adjacent channels. Based on the MAP decisions, a correlation metric between two adjacent channels can be computed. Let $Z_{\mathrm{lo}} = \{Z_{\mathrm{lo},k}\}_{k=1}^{\infty}$ and $Z_{\mathrm{hi}} = \{Z_{\mathrm{hi},k}\}_{k=1}^{\infty}$ denote the observation sequences for the lower and higher frequency channels, respectively. The observed sequences from n-sample realizations are denoted by z_{lo}^n and z_{hi}^n, respectively. The HMM parameter estimates ϕ_{lo} and ϕ_{hi} are obtained for the two channels using the Baum-Welch algorithm. Let $\hat{x}_{\mathrm{lo}}^n = \{\hat{x}_{\mathrm{lo},1}, \ldots, \hat{x}_{\mathrm{lo},n}\}$ and $\hat{x}_{\mathrm{hi}}^n = \{\hat{x}_{\mathrm{hi},1}, \ldots, \hat{x}_{\mathrm{hi},n}\}$ denote the corresponding decision sequences determined according to (19).

The normalized cross-correlation at zero lag between the sequences z_{lo}^n and z_{hi}^n is given by

$$\rho\left(z_{\mathrm{lo}}^n, z_{\mathrm{hi}}^n\right) = \frac{\left|\langle z_{\mathrm{lo}}^n, z_{\mathrm{hi}}^n \rangle\right|}{\|z_{\mathrm{lo}}^n\| \, \|z_{\mathrm{hi}}^n\|}, \tag{23}$$

where

$$\langle z_{\mathrm{lo}}^n, z_{\mathrm{hi}}^n \rangle = \sum_{k=1}^{n} z_{\mathrm{lo},k} z_{\mathrm{hi},k}^*, \tag{24}$$

denotes the Hermitian inner product between z_{lo}^n and z_{hi}^n, z^* denotes the complex conjugate of z, and $\|\cdot\|$ denotes the standard ℓ^2-norm. The normalized cross-correlation is bounded, i.e.,

$$0 \leq \rho\left(z_{\mathrm{lo}}^n, z_{\mathrm{hi}}^n\right) \leq 1. \tag{25}$$

However, for the purpose of channel aggregation, we require a correlation metric that takes into account the idle periods that coincide for the two channels. We denote the indicator function on the set or condition A by 1_A, and the indicator function for the complement of A by 1_{A^c}. Using this notation, we define modified observation sequences for the two channels by zeroing out the samples for which the PU is detected to be idle on both channels, i.e.,

$$\begin{aligned} \tilde{z}_{\mathrm{lo},k} &= z_{\mathrm{lo},k} \cdot 1_{\{\hat{x}_{\mathrm{lo},k} = \hat{x}_{\mathrm{hi},k} = 0\}^c}, \\ \tilde{z}_{\mathrm{hi},k} &= z_{\mathrm{hi},k} \cdot 1_{\{\hat{x}_{\mathrm{lo},k} = \hat{x}_{\mathrm{hi},k} = 0\}^c}, \end{aligned} \tag{26}$$

for $k = 1, \ldots, n$. The fraction of observation samples for which the PU is detected to be idle on both channels is given by

$$\gamma = \frac{1}{n} \sum_{k=1}^{n} 1_{\{\hat{x}_{\mathrm{lo},k} = \hat{x}_{\mathrm{hi},k} = 0\}}. \tag{27}$$

For such samples, the correlation should be assigned the value 1, indicating perfect correlation. The idle ratio is bounded, i.e.,

$$0 \leq \gamma \leq 1. \tag{28}$$

We then define a modified correlation metric as follows:

$$\tilde{\rho} = \gamma + (1 - \gamma) \rho\left(\tilde{z}_{\mathrm{lo}}^n, \tilde{z}_{\mathrm{hi}}^n\right). \tag{29}$$

It is easy to see from Eq. (25) and (28) that $0 \leq \tilde{\rho} \leq 1$. In our channel aggregation algorithm, two channels are merged if their correlation $\tilde{\rho}$, computed using (29), exceeds a threshold $\tilde{\rho}_{\min}$ (see Algorithm 2, line 7). When holes are combined, their MAP decisions must be combined as well. This combination of decisions is given by

$$\hat{x}_k = \begin{cases} 0, & \text{if } \hat{x}_{\mathrm{lo},k} = \hat{x}_{\mathrm{hi},k} = 0, \\ 1, & \text{otherwise.} \end{cases} \tag{30}$$

The PU in the combined channel is determined to be idle at time k if the PU in both subbands is determined to be idle at time k. Otherwise, the PU is determined to be active at time k.

G. Algorithm Descriptions

Parameter	Description
N_c	Number of channels at the finest sensing resolution
N_t	Number of filter taps for the channel selecting LPF
N_s	Number of samples in the sensing duration
N_i	Number of Baum-Welch iterations

TABLE I
ALGORITHM COMPLEXITY PARAMETERS.

A formal description of the proposed recursive wideband temporal sensing framework is given in Algorithm 1. The computational complexity is given by

$$O\left(N_c \log_2 N_c \cdot N_t N_s + N_c N_i N_s\right), \tag{31}$$

where the various parameters involved are shown in Table I. The terms of the complexity equation are derived as follows: $N_c \log_2 N_c$ is the number of nodes in the binary tree [27] and is therefore the maximum number of narrowband channels that can be sensed; $N_t N_s$ is the complexity of the filtering operation used to select a narrowband channel for sensing.

Algorithm 1 Wideband temporal sensing algorithm.

function RSense(f_c, W, W_r, $z^n_{\rm wb}$)
  if $W > W_r$ **then**
    $L_{\rm lo}$ = RSense($f_c - W/2, W/2, W_r, z^n_{\rm wb}$);
    $L_{\rm hi}$ = RSense($f_c + W/2, W/2, W_r, z^n_{\rm wb}$);
    if $L_{\rm hi}$ and $L_{\rm lo}$ are not empty **then**
      L = AggregateCh($L_{\rm hi}, L_{\rm lo}, z^n_{\rm wb}$);
    else
      L = empty list;
  else
    $h(n)$ = LPF(W, N_t);
    dec = Floor(W_0/W);
    z^n = DDC($z^n_{\rm wb}, f_c, h(n)$, dec);
    y^n = EnergyDet(z^n);
    $(\nu, G, \mu, R, \hat{x}^n)$ = BaumEst(y^n);
    π = StatDistr(G);
    if $\pi_1 > \pi_{\min,1}$ **then**
      L = list with single entry $(f_c, W, z^n, \hat{x}^n)$;
    else
      L = empty list;
  return L;

Algorithm 2 Aggregate channels.

function AggregateCh($L_{\rm hi}$, $L_{\rm lo}$, $z^n_{\rm wb}$)
  $(f_{{\rm lo},c}, W_{\rm lo}, z^n_{\rm lo}, \hat{x}^n_{\rm lo})$ = LowestCh($L_{\rm hi}$);
  $(f_{{\rm hi},c}, W_{\rm hi}, z^n_h, \hat{x}^n_h)$ = HighestCh($L_{\rm lo}$);
  L = CombineLists($L_{\rm hi}, L_{\rm lo}$);
  if $f_{{\rm hi},c} - W_{\rm hi}/2 == f_{{\rm lo},c} + W_l/2$ **then**
    ρ = Correlate($n, z^n_{\rm lo}, \hat{x}^n_{\rm lo}, z^n_{\rm hi}, \hat{x}^n_{\rm hi}$);
    if $\tilde{\rho} > \tilde{\rho}_{\min}$ **then**
      Remove($f_{{\rm lo},c}, W_{\rm lo}, z^n_{\rm lo}, \hat{x}^n_{\rm lo}$) and
        ($f_{{\rm hi},c}, W_{\rm hi}, z^n_{\rm hi}, \hat{x}^n_{\rm hi}$) from L;
      $h(n)$ = LPF($W_{\rm lo} + W_{\rm hi}, N_t$);
      dec = Floor($W_0/(W_{\rm lo} + W_{\rm hi})$);
      $f_c = f_{{\rm lo},c} + W_{\rm lo}/4 + W_{\rm hi}/4$;
      z^n = DDC($z^n_{\rm wb}, f_c, h(n)$, dec);
      $\hat{x}^n$ = Merge($\hat{x}^n_{\rm lo}$, $\hat{x}^n_{\rm hi}$);
      Add $(f_c, W_{\rm lo} + W_{\rm hi}, z^n, \hat{x}^n)$
        to L;
  return L;

The term $N_i N_s$ represents the per-channel complexity of the Baum-Welch algorithm.

We shall not formally describe any of the other functions used in Algorithms 1 and 2, but basic descriptions will be given. The function AggregateCh($L_{\rm hi}, L_{\rm lo}, z^n_{\rm wb}$), as specified in Algorithm 2, determines whether two adjacent holes should be combined. The function Correlate($n, z^n_{\rm lo}, \hat{x}^n_{\rm lo}, z^n_{\rm hi}, \hat{x}^n_{\rm hi}$) computes the modified correlation metric given by (29). The function LPF(W) designs a finite impulse response (FIR) lowpass filter with bandwidth W. The function DDC($z^n_{\rm wb}, f_c, h(n)$, dec) performs channelization as discussed in Section IV-B. The wideband signal z^n_{wb} is mixed down by center frequency f_c, lowpass filtered by a FIR filter with discrete taps $h(n)$, and decimated by dec. The function EnergyDet(z^n) performs energy detection based on the processed received power samples given in (11).

The function BaumEst(y^n) estimates the parameter of the PU in the selected narrowband channel with processed received power samples, y^n, using the Baum-Welch algorithm as summarized in Section IV-D. The function StatDistr(G) computes the stationary state distribution corresponding to the transition matrix G using (20). The functions HighestCh(L) and LowestCh(L) select the highest-frequency narrowband channel and the lowest-frequency narrowband channel, respectively, from a list of estimated channel parameters L. The function CombineLists(L_1, L_2) merges two lists of estimated channel parameters into a single list and sorts the list in decreasing order of center frequency. The function Merge($\hat{x}^n_{\rm lo}$, $\hat{x}^n_{\rm hi}$) combines the MAP decisions from the two channels as in (30).

V. Simulation and Numerical Results

A. Simulation 1: Comparison of Techniques

We tested the wideband energy detector, the wideband edge detector, and the proposed wideband temporal spectrum detector against OFDM and GMSK signals with duty cycles varying among 1.0, 0.5, 0.25, and 0.125. We used an energy detection averaging window of $N_{\rm avg} = 1$ samples. We assumed a minimum duty cycle $\pi_{\min,1} = 0.1$ and a minimum modified correlation threshold for combining channels of $\tilde{\rho}_{\min} = 0.7$. For each modulation scheme and duty cycle tested, a wideband capture was generated with signals of random center frequency and symbol rate over a 10 MHz band. We used a minimum sensing resolution of 10 kHz, resulting in a search tree depth of $d = 10$. The modulated data on the signals was generated by a uniform random number generator. All of the signals were received through a simulated AWGN and Rayleigh fading channel with 10 dB SNR and used the currently tested modulation and duty cycle. A total of 10,000 simulation iterations were performed for each modulation and duty cycle pair.

Wideband signals were also generated specifically for plotting qualitative results. These wideband signals contained 4 narrowband signals with 1 MHz bandwidth and carrier spacing of 2 MHz. The four signals have duty cycles of 1.0, 0.5, 0.25, and 0.125 from lowest-frequency to highest-frequency. All highlighted PSD plots in this paper show the results of applying a wideband sensing algorithm to one of these wideband signals, where the shaded areas are the detected holes and the white areas are the detected signals.

B. Simulation 2: Performance at Varying SNR

To test the performance of the proposed wideband temporal detector, we tested the detector against OFDM and GMSK signals with duty cycle of 0.125 and SNR ranging between -20 and 20 dB. We varied the energy detection window size, $N_{\rm avg}$, among 1, 10, 100, and 1000 samples. We assumed a minimum duty cycle $\pi_{\min,1} = 0.1$ and a minimum modified correlation threshold for combining channels of $\tilde{\rho}_{\min} = 0.7$. For each modulation scheme, a wideband capture was generated with signals of random center frequency and symbol rate over a 10 MHz band. We used a minimum sensing resolution of 10 kHz, resulting in a search tree depth of $d = 10$. The

modulated data on the signals was generated by a uniform random number generator. All of the signals were received through a simulated AWGN and Rayleigh fading channel. A total of 10,000 simulation iterations were performed for each modulation and energy detection window.

C. Simulation 1 Results: Qualitative Comparison of Techniques

Qualitative results of the proposed wideband temporal sensing algorithm are depicted in Fig. 7 for OFDM and Fig. 8 for GMSK. Shaded areas represent detected spectrum holes. It can be seen that the proposed wideband temporal spectrum detector performed well for all tested duty cycles and both simulated modulation schemes. The qualitative simulation results of the proposed spectrum detector can be compared to the qualitative results from Section II. Comparing Fig. 7 to Figs. 1 and 3 shows that reducing the duty cycle does not degrade the performance of the proposed detector for OFDM like it does for wideband energy detection. Similarly, comparing Fig. 8 to Figs. 2 and 4 shows that the proposed detector is also not degraded by reduced duty cycles for GMSK. Furthermore, comparing Fig. 8 to Fig. 4 shows that the smooth band edges of GMSK do not degrade the performance of the proposed detector like they do for the wideband energy detector.

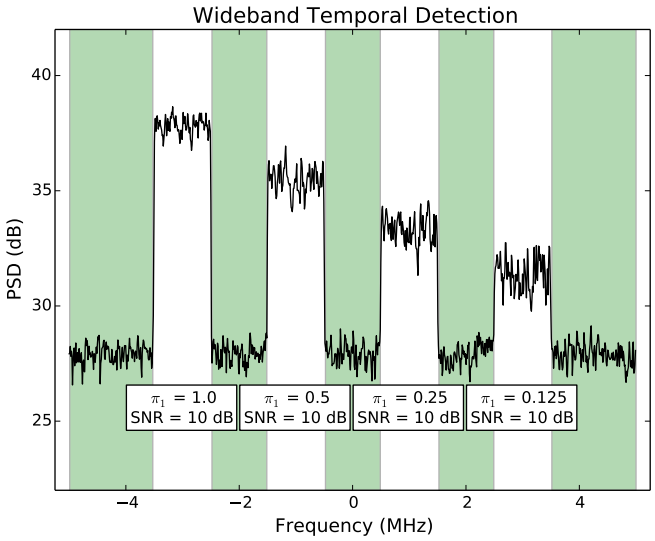

Fig. 7. Results of wideband temporal spectrum detector for OFDM signals with 10 dB SNR and 100%, 50%, 25%, and 12.5% duty cycles.

D. Simulation 1 Results: Quantitative Comparison of Techniques

Quantitative sensing results are depicted by ROC (receiver operating characteristic) curves generated by the simulation. The probability of true detect, defined as the proportion of trials in which the detector correctly indentified that an active PU was transmitting, is plotted against the probability of false detect, defined as the proportion of trials in which the detector incorrectly indentified an idle PU to be an active PU. The ROC curves represent the average detector performance over

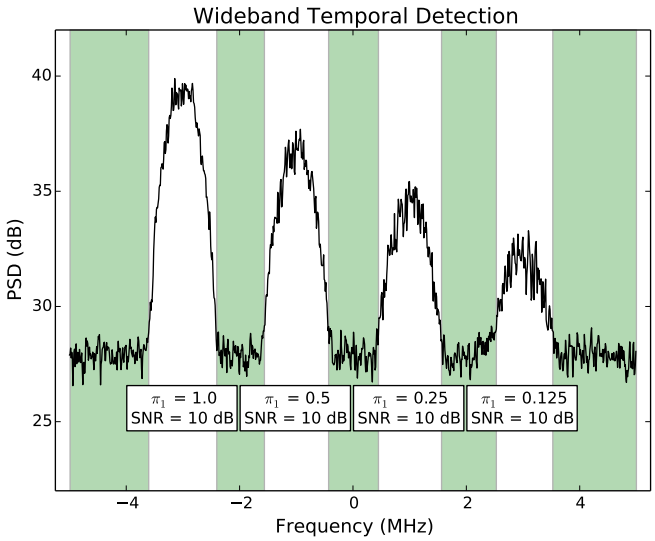

Fig. 8. Results of wideband temporal spectrum detector for GMSK signals with 10 dB SNR and 100%, 50%, 25%, and 12.5% duty cycles.

many random wideband captures using the same modulation, duty cycle, and SNR. Performance of the wideband energy detector is shown in Fig. 9 for OFDM and Fig. 10 for GMSK. Performance of the wideband edge detector is shown in Fig. 11 for OFDM and Fig. 12 for GMSK. In the wideband energy and edge detector results, it can clearly be observed that detector performance degrades as PU duty cycle decreases. In the case of GMSK, the performance of the wideband edge detector is substantially degraded, due to the edge detector's hindered ability to detect gradual changes. Performance of the wideband temporal spectrum detector is shown in Fig. 13 for OFDM and Fig. 14 for GMSK. It is clear from these results that the proposed detector's performance was not significantly degraded by reduced duty cycles.

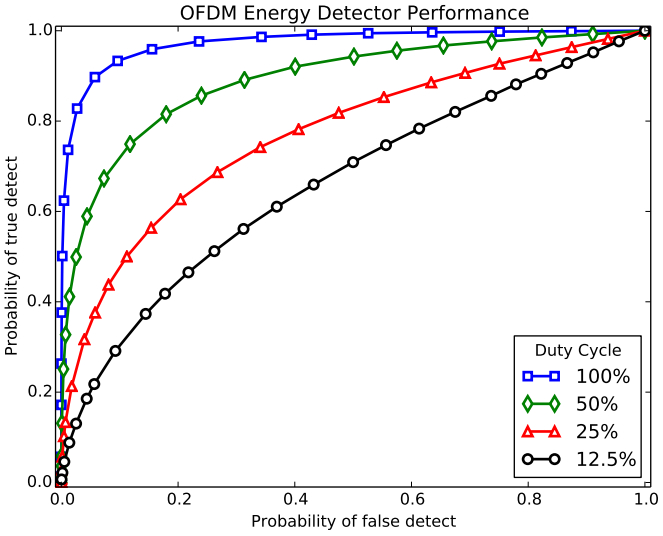

Fig. 9. ROC curve for wideband energy detector for OFDM signals with 10 dB SNR and 100%, 50%, 25%, and 12.5% duty cycles.

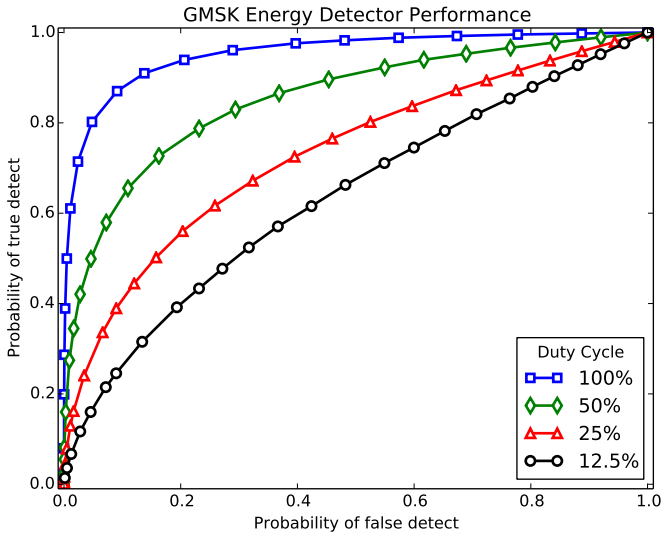

Fig. 10. ROC curve for wideband energy detector for GMSK signals with 10 dB SNR and 100%, 50%, 25%, and 12.5% duty cycles.

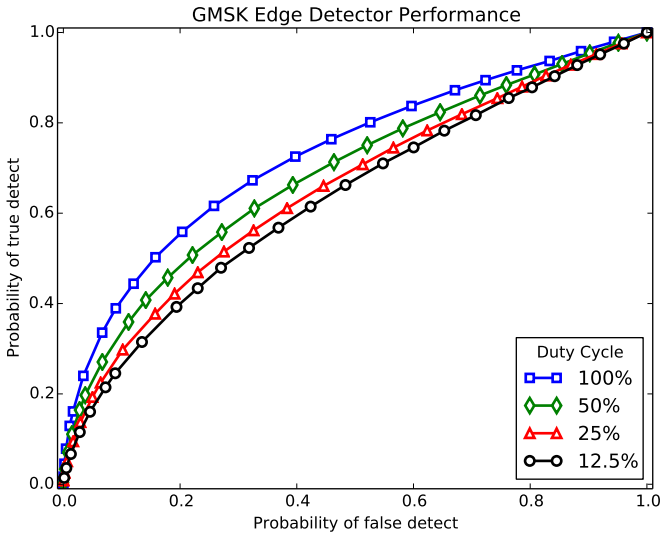

Fig. 12. ROC curve for wideband edge detector for GMSK signals with 10 dB SNR and 100%, 50%, 25%, and 12.5% duty cycles.

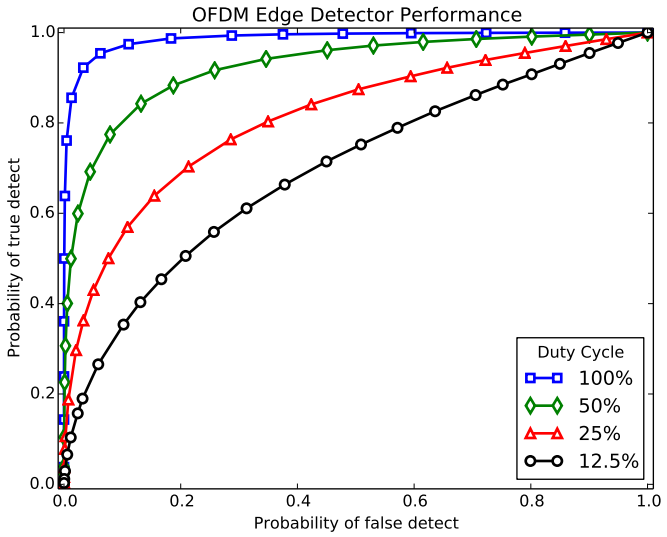

Fig. 11. ROC curve for wideband edge detector for OFDM signals with 10 dB SNR and 100%, 50%, 25%, and 12.5% duty cycles.

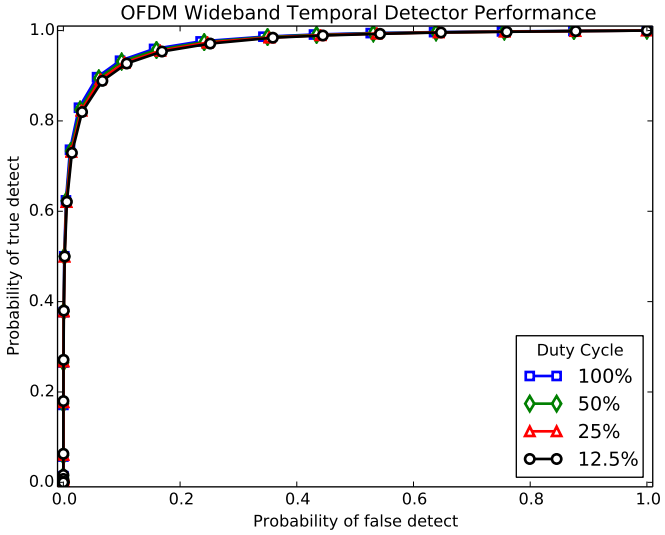

Fig. 13. ROC curve for wideband temporal spectrum detector for OFDM signals with 10 dB SNR and 100%, 50%, 25%, and 12.5% duty cycles.

E. Simulation 2 Results

For simulation 2, false alarm and true positive rates were collected for a variety of thresholds at all tested SNR and energy detection windows. To impose many ROC curves onto a single plot, true positive rate at a constant false alarm rate (CFAR) of 0.01 is shown. In Fig. 15, the true positive rate for a CFAR of 0.01 is shown for the proposed detector against OFDM signals with duty cycle of 0.125 and varying SNR. In Fig. 16, the true positive rate is shown for GMSK signals. As the energy detection window increases, the sensitivity of the detector increases. However, increasing energy detector length increases the likelihood that samples from idle and busy cycles are averaged together, degrading detector performance.

VI. Conclusion

The proposed wideband temporal spectrum sensing framework performed comparably for bursting signals with various duty cycles to the wideband energy detector applied to signals with 100% duty cycle. In the case of bursting signals, the recursive wideband temporal spectrum sensing algorithm proved to be much more robust than the frequency-only sensing algorithms. The power of the proposed sensing algorithm comes at the cost of computation time: $O(N_c \log_2 N_c)$ narrowband sensing operations must be performed, as well as FIR filtering for channel selection. We suggest that a cognitive radio would use this wideband sensing algorithm during initialization and revert to narrowband or multiband sensing once the set of PU channels for temporal sensing has been determined. The Baum-Welch algorithm may continue

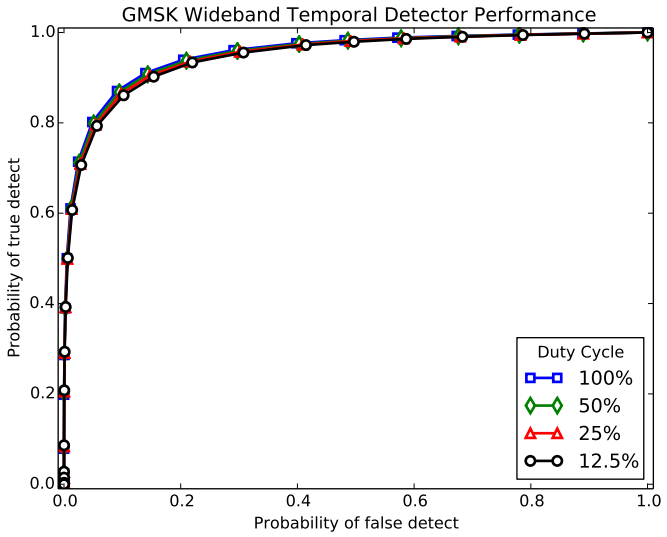

Fig. 14. ROC curve for wideband temporal spectrum detector for GMSK signals with 10 dB SNR and 100%, 50%, 25%, and 12.5% duty cycles.

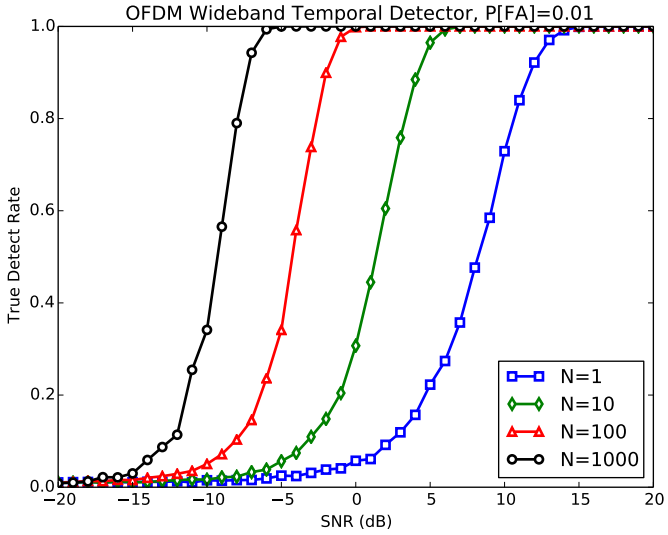

Fig. 15. CFAR curves for wideband temporal spectrum detector for OFDM signals with duty cycle of 12.5%, SNR ranging from -20 to 20 dB, and energy detection window of 1, 10, 100, or 1000 samples.

to be leveraged, in the narrowband or multiband case, both for refining parameter estimation and prediction of future PU state. To accommodate time-varying RF environments, an SU can alternate between wideband temporal sensing for channel acquisition and multiband sensing for PU tracking.

Several extensions of the proposed wideband temporal spectrum sensing algorithm could be explored further. To reduce overall computation, use of a frequency-domain channelizer that allows the channel selection operators to share filter computations and leverages heavily optimized implementations for the FFT could be investigated. To improve PU state detection and prediction accuracy for a wider range of PU behaviors, the HMM could be extended to a hidden bivariate Markov model [17], which has phase-type, rather than geometric state sojourn time distributions. In the present

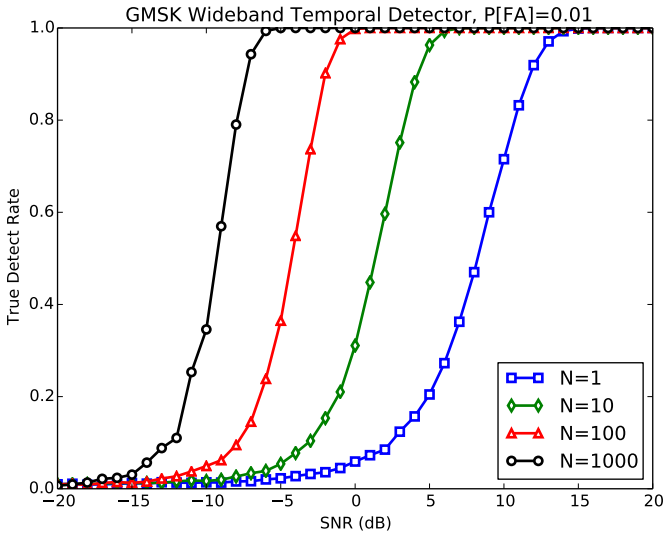

Fig. 16. CFAR curves for wideband temporal spectrum detector for GMSK signals with duty cycle of 12.5%, SNR ranging from -20 to 20 dB, and energy detection window of 1, 10, 100, or 1000 samples.

paper, a simple energy detector was used as a front-end for the HMM-based parameter estimator and state detector. Even with the performance gain that could be achieved by extending our scheme using a hidden bivariate Markov model, detection of a PU at very low SNR using an energy detector may perform poorly. For such low SNR scenarios, better performance could be achieved by means of a matched filter or cyclostationary detector in conjunction with the recursive channel search.

ACKNOWLEDGEMENT

The authors would like to thank the Editor and the anonymous reviewers for helpful comments that helped to improve the presentation of this paper.

REFERENCES

[1] J. M. Bruno and B. L. Mark, "A recursive algorithm for joint time-frequency wideband spectrum sensing," in *IEEE 2015 Wireless Communications and Networking Conference Workshops (WCNCW), International Workshop on Smart Spectrum*, New Orleans, LA, March 2015, pp. 235–240.

[2] FCC, "Spectrum policy task force," Rep. ET Docket, Federal Communications Commission, Tech. Rep. 02-135, Nov. 2002.

[3] S. Haykin, "Cognitive radio: Brain-empowered wireless communications," *IEEE J. Sel. Areas Commun.*, vol. 23, no. 2, pp. 201–220, Sep. 2006.

[4] T. Yucek and H. Arslan, "A survey of spectrum sensing algorithms for cognitive radio applications," *IEEE Commun. Surveys Tuts.*, vol. 11, no. 1, pp. 116–130, March. 2009.

[5] W. A. Gardner, "Exploitation of spectral redundancy in cyclostationary signals," *IEEE Signal Process. Mag.*, vol. 8, no. 2, pp. 14–36, April 1991.

[6] A. Mariani, A. Giorgetti, and M. Chiani, "Wideband spectrum sensing by model order selection," *IEEE Trans. Wireless Commun.*, vol. 14, no. 12, pp. 6710–6721, Dec 2015.

[7] R. Lopez-Valcarce and G. Vazquez-Vilar, "Wideband spectrum sensing in cognitive radio: Joint estimation of noise variance and multiple signal levels," in *IEEE 10th Workshop on Signal Processing Advances in Wireless Communications (SPAWC'09)*, June 2009, pp. 96–100.

[8] M. Sanna and M. Murroni, "Opportunistic wideband spectrum sensing for cognitive radios with genetic optimization," in *2010 IEEE International Conference on Communications (ICC)*, May 2010, pp. 1–5.

[9] T. H. Yu, S. Rodriguez-Parera, D. Markovic, and D. Cabric, "Cognitive radio wideband spectrum sensing using multitap windowing and power detection with threshold adaptation," in *2010 IEEE International Conference on Communications (ICC)*, May 2010, pp. 1–6.

[10] D. Bao, L. D. Vito, and S. Rapuano, "A histogram-based segmentation method for wideband spectrum sensing in cognitive radios," *IEEE Trans. Instrum. Meas.*, vol. 62, no. 7, pp. 1900–1908, July 2013.

[11] L. Angrisani, G. Betta, D. Capriglione, G. Cerro, L. Ferrigno, and G. Miele, "Proposal and analysis of new algorithms for wideband spectrum sensing in cognitive radio," in *2014 IEEE International Instrumentation and Measurement Technology Conference (I2MTC)*, May 2014, pp. 701–706.

[12] Z. Tian and G. B. Giannakis, "A wavelet approach to wideband spectrum sensing for cognitive radios," in *1st Int. Conf. on Cog. Radio Oriented Wireless Nets. and Comms. (CROWNCOM)*, June 2006, pp. 1–5.

[13] H. Sun, A. Nallanathan, S. Cui, and C.-X. Wang, "Cooperative wideband spectrum sensing over fading channels," *IEEE Trans. Veh. Technol.*, vol. 65, no. 3, pp. 1382–1394, 2016.

[14] Z. Tian and G. Giannakis, "Compressed sensing for wideband cognitive radios," in *IEEE International Conference on Acoustics, Speech and Signal Processing (ICASSP'07)*, vol. 4, April 2007, pp. IV–1357–IV–1360.

[15] A. Mariani, S. Kandeepan, and A. Giorgetti, "Periodic spectrum sensing with non-continuous primary user transmissions," *IEEE Trans. Wireless Commun.*, vol. 14, no. 3, pp. 1636–1649, March 2015.

[16] I. Akbar and W. Tranter, "Dynamic spectrum allocation in cognitive radio using hidden markov models: Poisson distributed case," in *IEEE SoutheastCon 2007*, March 2007, pp. 196–201.

[17] T. Nguyen, B. L. Mark, and Y. Ephraim, "Spectrum sensing using a hidden bivariate Markov model," *IEEE Trans. Wireless Commun.*, vol. 12, no. 9, pp. 4582–4591, Aug. 2013.

[18] P. Tehrani, L. Tong, and Q. Zhao, "Asymptotically efficient multichannel estimation for opportunistic spectrum access," *IEEE Trans. Signal Process.*, vol. 60, no. 10, pp. 5347–5360, Oct. 2012.

[19] Q. Zhao, L. Tong, A. Swami, and Y. Chen, "Decentralized cognitive mac for opportunistic spectrum access in ad hoc networks: A pomdp framework," *IEEE J. Sel. Areas Commun.*, vol. 25, no. 3, pp. 589–600, April 2007.

[20] FCC Online Table of Frequency Allocations, https://transition.fcc.gov/oet/spectrum/table/fcctable.pdf, accessed: 8-31-2017.

[21] M. H. Hayes, *Statistical Digital Signal Processing and Modeling*, 1st ed. New York, NY, USA: John Wiley & Sons, Inc., 1996.

[22] D. Cabric, S. Mishra, and R. Brodersen, "Implementation issues in spectrum sensing for cognitive radios," in *Thirty-Eighth Asilomar Conference on Signals, Systems and Computers*, vol. 1, Nov 2004, pp. 772–776 Vol.1.

[23] O. Olabiyi and A. Annamalai, "Extending the capability of energy detector for sensing of heterogeneous wideband spectrum," in *IEEE Consumer Comm. and Net. Conf. (CCNC'12)*, Jan 2012, pp. 454–458.

[24] H. Sun, A. Nallanathan, C.-X. Wang, and Y. Chen, "Wideband spectrum sensing for cognitive radio networks: A survey," *IEEE Wireless Communications*, vol. 20, no. 2, pp. 74–81, April 2013.

[25] S. K. Sharma, S. Chatzinotas, and B. Ottersten, "Compressive sparsity order estimation for wideband cognitive radio receiver," *IEEE Trans. Signal Process.*, vol. 62, no. 19, pp. 4984–4996, Oct 2014.

[26] Y. Ephraim and N. Merhav, "Hidden Markov processes," *IEEE Trans. Inf. Theory*, vol. 48, no. 6, pp. 1518–1569, June 2002.

[27] D. Knuth, *The Art of Computer Programming, Vol. 1: Fundamental Algorithms*, 3rd ed. Addison-Wesley, 1997.

[28] F. J. Harris and C. Dick, "Performing simultaneous arbitrary spectral translation, and sample rate change in polyphase interpolating or decimating filters in transmitters and receivers," in *Software Defined Radio Conference*, San Diego, California, 2002, pp. 11–12.

[29] F. J. Harris, *Multirate Signal Processing for Communication Systems*. Upper Saddle River, NJ, USA: Prentice Hall PTR, 2004.

[30] Y. Sun, B. L. Mark, and Y. Ephraim, "Online parameter estimation for temporal spectrum sensing," *IEEE Trans. on Wireless Commun.*, vol. 14, no. 8, pp. 4105–4114, Aug. 2015.

[31] L. E. Baum and T. Petrie, "Statistical inference for probabilistic functions of finite state Markov chains," *Annals of Mathematical Statistics*, vol. 37, no. 6, pp. 1554–1563, Apr. 1966.

[32] T. M. Cover and J. A. Thomas, *Elements of Information Theory*. Wiley-Interscience, 2006.

Joseph M. Bruno (S'10-M'12) received the Ph.D. in Electrical Engineering from George Mason University in 2017, the M.S. in Electrical Engineering from Johns Hopkins University in 2013, and the B.S. degree in Electrical Engineering with a minor in Computer Science from the University of Delaware in 2011. He is a senior member of the professional staff at the Johns Hopkins Applied Physics Lab. His research interests include digital communications and signal processing, software-defined radio, and machine learning.

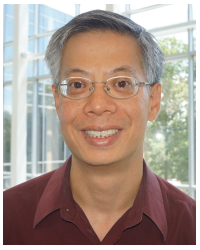

Brian L. Mark (S'91-M'95-SM'08) received the Ph.D. in Electrical Engineering from Princeton University in 1995 and the B.A.Sc. degree in Computer Engineering with an option in Mathematics from the University of Waterloo in 1991. He was a Research Staff Member at the C&C Research Laboratories, NEC USA, from 1995 to 1999. In 1999, he was on part-time leave from NEC as a visiting researcher at Ecole Nationale Supérieure des Télécommunications in Paris, France. In 2000, he joined George Mason University, where he currently is Professor of Electrical and Computer Engineering. He served as acting chair of the Dept. of Bioengineering from 2015-2017. He was an associate editor for IEEE Transactions on Vehicular Technology from 2006-2009. His main research interests lie in the design and performance analysis of communication networks.